# Ultrafast laser-pulse control for selective excitation of high vibrational states and dissociation of diatomic molecules in an environment

M. V. Korolkov and G. K. Paramonov*
*Institut für Physikalische und Theoretische Chemie, Freie Universität Berlin, WE 3, Takustrasse 3, D-14195 Berlin, Germany*
(Received 24 February 1997)

Ultrafast state-selective vibrational excitation and dissociation controlled by shaped subpicosecond infrared laser pulses is investigated within the reduced density matrix formalism beyond a Markov-type approximation for diatomic molecules, which are coupled to an unobserved quasiresonant environment. Dissipative quantum dynamics in a classical electric field is simulated for discrete vibrational bound states and for dissociative continuum states of a one-dimensional dissociative Morse oscillator, tailored to the local OH bond of the $H_2O$ and HOD molecules in the electronic ground state. Flexible laser control schemes are developed and demonstrated on a picosecond time scale, which enable one either to localize the population at prescribed high-lying discrete vibrational levels of OH, up to those close to the dissociation threshold, with the probability up to 70–80 % without substantial dissociation or, alternatively, achieve the dissociation yield of about 75%, while the strength of the quasiresonant molecule-environment coupling results in subpicosecond lifetimes of the vibrational bound states. The optimal laser control schemes may include the superposition of up to four subpicosecond laser pulses. [S1050-2947(97)02710-8]

PACS number(s): 42.50.Vk

## I. INTRODUCTION

Laser-controlled manipulation of population dynamics of molecules, in particular complete localization of population at a prescribed target level, or the population transfer, has long been a subject of considerable attention [1–31]. An important line in this field is ultrafast state-selective control of vibrational excitation and dissociation of molecules, which may result in various types of intermolecular and intramolecular selectivity [32–41], if the process of selective steering of a molecule to a specified target by the laser field can compete against nonselective processes, such as relaxation [15,25–31]. Of special interest is the problem of state-selective preparation of molecules at high vibrational levels, including levels close to the dissociation threshold [38,39], which is important for controlling cross sections in molecular collisions, for manipulating the outcome of chemical reactions, and creates favourable starting conditions for efficient dissociation.

Until now, theoretical investigations of the state-selective vibrational excitation have been mostly devoted to low levels of isolated molecules, including fairly realistic one-dimensional (1D), 2D, and 3D models of OH, HF, HOD, $H_2O$, $SiH_2$, and $NH_2$ molecules [6,11,17–20,22]. The adiabatic passage approach for the population transfer has been studied both theoretically [10,13,14,24,27] and experimentally [4,5,9,12,21,28]. The role of the environmental degrees of freedom has been studied in Markov-type approximations [15,25,26] and recently within a non-Markov approach [29–31]. It has been shown, in particular for low vibrational states of OH [31], that the non-Markov approach provides 20–30 % higher level of the population transfer on a picosecond (ps) time scale. Selective preparation of high vibrational bound states, including those close to the dissociation threshold, have been simulated only for isolated OH [38,39], neglecting the coupling to an environment. The laser-induced dissociation of molecules has also attracted much interest (see, for example, recent works [39–41], and references therein), but to the best of our knowledge, the environmental degrees of freedom have not been taken into account yet.

The aim of the present work is to investigate the possibility of ultrafast localization of population at very high vibrational levels of diatomic molecules, up to the levels close to the dissociation threshold, along with the laser-induced dissociation from selectively prepared high vibrational bound states in the presence of an environment.

As a model system in our computer simulations we use a dissociative, one-dimensional quantum Morse oscillator, with the specific parameters being tailored to the local OH bond of the $H_2O$ and HOD molecules in the electronic ground state. The Morse oscillator (a molecule) is coupled to a thermal bath (an unobserved environment) represented by an infinite number of harmonic oscillators. In order to investigate the possibility of state-selective laser control and dissociation at the extreme conditions, the environment is assumed to be quasiresonant, with the maximal strength of the coupling to the molecule corresponding exactly to molecular frequencies. Similar quasiresonant model environments have been already used in our previous works [29–31] for investigation of state-selective excitation of low vibrational states of HOD molecules [29], ultrafast laser-pulse control of isomerization reactions [30], and for selective vibrational excitation of OH up to $v=10$ [31], where dissociation could be safely neglected [38]. The laser field is treated classically and is assumed to excite molecular vibrations without influence on the environment. Molecular rotations, coupling of the dissociation fragments to the environment, and the laser-

*Permanent address: B. I. Stepanov Institute of Physics, Belarus Academy of Sciences, Skaryna Ave. 70, 220602 Minsk, Republic of Belarus.

 

induced continuum-continuum transitions are not taken into account. These assumptions are discussed in the following. All results presented below have been simulated beyond a Markov-type approximation.

## II. MODELS, EQUATIONS OF MOTION AND TECHNIQUES

The Hamiltonian characterizing the total system, a molecule coupled to an environment, can be written in the form

$$\mathcal{H}(r,\{z_u\},t)=\mathcal{H}_{\rm mol}(r)+V(r,t)+W(r,\{z_u\})+\mathcal{H}_e(\{z_u\}), \tag{1}$$

where $\mathcal{H}_{\rm mol}(r)$ is the Hamiltonian of an unperturbed molecule, $V(r,t)$ describes its interaction with a laser field, $W(r,\{z_u\})$ describes the interaction between the molecule and the environment, and $\mathcal{H}_e(\{z_u\})$ is the Hamiltonian for the environment, with $\{z_u\}$ standing for the environmental degrees of freedom. Atomic units are used below unless otherwise explicitly indicated.

An unperturbed diatomic molecule is described by the molecular Hamiltonian

$$\mathcal{H}_{\rm mol}(r)=p^2/2m+V_M(r), \tag{2}$$

where for OH under study the reduced mass is $m=1728.539m_e$, with $m_e$ standing for electron rest mass, and the Morse potential is specified by

$$V_M(r)=D\{\exp[-2\beta(r-r_0)]-2\exp[-\beta(r-r_0)]\}, \tag{3}$$

where the equilibrium distance $r_0=1.821a_0$, Morse parameter $\beta=1.189a_0^{-1}$, $a_0$ is the Bohr radius, and well depth $D=0.1994E_h$.

The discrete, bound molecular eigenstates are denoted as $|v\rangle$. The molecular Hamiltonian $\mathcal{H}_{\rm mol}(r)$ supports 22 bound vibrational eigenstates with eigenenergies

$$E_v=-D+\hbar[\omega_e(v+0.5)-\Delta^a(v+0.5)^2], \tag{4}$$

where $v=0,1,\ldots,v_{\max}=21$, the harmonic frequency is $\omega_e=\beta\sqrt{2D/m}$, and the anharmonicity constant is $\Delta^a=\hbar\omega_e^2/4D$. The eigenfunctions $|v\rangle$ of the bound vibrational states are the well-known Morse oscillator wave functions (see, e.g., Refs. [42,43]).

The continuum eigenstates with eigenenergies $\varepsilon>0$ are denoted as $|\varepsilon\rangle$, and the eigenfunctions $\psi(\varepsilon,r)$ of the continuum states may be represented by the Whittaker functions (see, e.g., Ref. [44]).

The molecular eigenstates satisfy the time-independent Schrödinger equations

$$\mathcal{H}_{\rm mol}(r)|v\rangle=E_v|v\rangle,\quad \mathcal{H}_{\rm mol}(r)|\varepsilon\rangle=\varepsilon|\varepsilon\rangle \tag{5}$$

and the orthonormalization relations

$$\langle v|v'\rangle=\delta_{vv'},\quad \langle\varepsilon|\varepsilon'\rangle=\delta(\varepsilon-\varepsilon'),\quad \langle\varepsilon|v\rangle=0. \tag{6}$$

A laser field is assumed to be linearly polarized. Its interaction with the molecule is described within the semiclassical electric dipole approximation by the interaction Hamiltonian

$$V(r,t)=-\mu(r)\mathcal{E}(t), \tag{7}$$

where $\mathcal{E}(t)$ is the component of the laser electric field strength along the molecular dipole, and the molecular dipole moment operator is represented by Mecke function [45,46]

$$\mu(r)=\mu_0 r\,\exp(-r/r^0), \tag{8}$$

where $\mu_0=7.85\,D/\text{Å}$ and $r^0=0.6$ Å.

The Hamiltonian $W(r,\{z_u\})$, describing the coupling of the molecule to an environment, is taken in the form

$$W(r,\{z_u\})=\Lambda Q(r)F(\{z_u\}), \tag{9}$$

where $\Lambda$ is a constant for the strength of the molecule-environment coupling, and $Q(r)$ and $F(\{z_u\})$ are the molecular and the environment coupling operators, correspondingly.

The molecular coupling operator is chosen in the form [47]

$$Q(r)=(1/\beta)\{1-\exp[-\beta(r-r_0)]\}, \tag{10}$$

as in our previous work [31].

The environmental coupling operator $F(\{z_u\})$ is assumed to be linear and factorized with respect to the environmental degrees of freedom $z_u$ as

$$F(\{z_u\})=\sum_u K_u z_u,\quad u=1,2,\ldots\ . \tag{11}$$

The molecule-environment coupling operator (9) is nonlinear, but it becomes linear,

$$W(r,\{z_u\})\to\Lambda(r-r_0)\sum_u K_u z_u, \tag{12}$$

in the harmonic limit for the Morse oscillator: $D\to\infty$, $\beta\to 0$, and $D\beta^2\to$const.

The Hamiltonian for the environment $\mathcal{H}_e(\{z_u\})$ is represented by an infinite ensemble of harmonic oscillators:

$$\mathcal{H}_e(\{z_u\})=\sum_u \mathcal{H}_u(z_u), \tag{13}$$

where

$$\mathcal{H}_u(z_u)=p_u^2/2m_u+(m_u/2)\Omega_u^2 z_u^2, \tag{14}$$

with $m_u$ being the effective mass and $\Omega_u$ being the frequency of the environmental oscillator $u$, where $u=1,2,\ldots$ . The eigenfunctions corresponding to the environmental degrees of freedom are the well-known harmonic-oscillator wave functions.

It is suitable to start with the equation of motion for the total system (molecule plus environment) in the interaction picture. The density matrix characterizing the total system in the interaction picture is denoted by $\sigma_I(t)$. Its time evolution is governed by the Liouville equation [48]

$$\frac{\partial\sigma_I(t)}{\partial t}=(i/\hbar)\mathcal{E}(t)[\mu_I(r,t),\sigma_I(t)]-i(\Lambda/\hbar)\times[Q_I(r,t)F_I(\{z_u\},t),\sigma_I(t)]. \tag{15}$$

The reduced density matrix of the molecule coupled to an unobserved environment is defined as

$$\varrho_I(t)=\mathrm{Tr}_e[\sigma_I(t)], \tag{16}$$

where $\mathrm{Tr}_e$ refers to the trace over all environmental degrees of freedom. The equation of motion for the reduced density matrix is obtained, as usual, (see, e.g., Ref. [48]) by making use of the formal solution of the Liouville equation (15),

$$\sigma_I(t)=\sigma_I(0)+(i/\hbar)\int_0^t dt'\{[\mathcal{E}(t')\mu_I(r,t'),\sigma_I(t')] - \Lambda[Q_I(r,t')F_I(\{z_u\},t'),\sigma_I(t')]\}, \tag{17}$$

substituting Eq. (17) back into Eq. (15), and evaluating the trace (16) under the basic condition of irreversibility

$$\sigma_I(t)=\varrho_I(t)\varrho_e(0), \tag{18}$$

where

$$\varrho_e(0)=\exp(-\mathcal{H}_e/k_BT)/\mathrm{Tr}_e[\exp(-\mathcal{H}_e/k_BT)]. \tag{19}$$

Finally one gets the equation of motion for the reduced density matrix

$$\frac{\partial\varrho_I(t)}{\partial t}=(i/\hbar)\mathcal{E}(t)[\mu_I(r,t),\varrho_I(t)] - (\Lambda/\hbar)^2[Q_I(r,t),G_I(r,t)], \tag{20}$$

where $G_I(r,t)$, which will be referred to as the time-dependent relaxation matrix, is given in the interaction picture by

$$G_I(r,t)=\int_0^t dt'\{Q_I(r,t')\varrho_I(t')\langle F(t)F(t')\rangle - \varrho_I(t')Q_I(r,t')\langle F(t')F(t)\rangle\}, \tag{21}$$

and the time correlation functions $\langle F(t)F(t')\rangle$ and $\langle F(t')F(t)\rangle$ in Eq. (21) are defined, as usual [48] by

$$\langle F(t)F(t')\rangle=\mathrm{Tr}_e[F_I(\{z_u\},t)F_I(\{z_u\},t')\varrho_e(0)], \tag{22}$$

$$\langle F(t')F(t)\rangle=\mathrm{Tr}_e[F_I(\{z_u\},t')F_I(\{z_u\},t)\varrho_e(0)]. \tag{23}$$

For the model environment composed of an infinite ensemble of harmonic oscillators [see Eqs. (13) and (14)] it can be shown that

$$\langle F(t)F(t')\rangle=\frac{1}{2}\sum_u(\hbar/m_u\Omega_u)K_u^2\Phi(\Omega_u,t-t',T), \tag{24}$$

where

$$\Phi(\Omega_u,t-t',T)=\{[\overline{n(}\Omega_u)+1]\exp[-i\Omega_u(t-t')] + \overline{n(}\Omega_u)\exp[i\Omega_u(t-t')]\}, \tag{25}$$

with

$$\overline{n(}\Omega_u)=\frac{1}{\exp(\hbar\Omega_u/k_BT)-1}, \tag{26}$$

and $\langle F(t)F(t')\rangle=\langle F(t')F(t)\rangle^*$. It is also suitable to assume in Eq. (24) that $(\hbar/m_u\Omega_u)=a_0^2$, which yields the environment coupling $F(\{z_u\})$ of the same order of magnitude as the molecular coupling $Q(r)$. The specific values of the parameters $K_u$ and $\Omega_u$ in Eqs. (24)–(26) are still rather arbitrary and flexible, they should be defined by a particular environment and the molecule-environment coupling, for example, such as described below for a model quasiresonant environment.

The quasiresonant nature of the molecule-environment coupling is taken into account, as in our previous work [31], under the assumption that the environmental frequencies $\Omega_u$ are closely spaced near the molecular frequencies $\omega_{mn}=(E_m-E_n)/\hbar$, and the density of the environmental frequencies in the vicinity of each $\omega_{mn}$ is represented by a Lorentzian-type distribution

$$g_{mn}(\Omega)=\frac{1}{\pi}(\gamma_{mn}/\Omega_0)^p\frac{\gamma_{mn}}{\gamma_{mn}^2+(\omega_{mn}-\Omega)^2}, \tag{27}$$

where $(\gamma_{mn}/\Omega_0)^p$ is a normalization factor with a scaling parameter $\Omega_0$, and $\gamma_{mn}>0$ determines the width of the distribution $g_{mn}(\Omega)$ which has a maximum at $\Omega=\omega_{mn}$. Under these assumptions we can change in Eq. (24) from the infinite sum over $u$ to finite sums over $m>n$ containing the integrals

$$\langle F(t)F(t')\rangle=\frac{a_0^2}{2}\sum_u K_u^2\Phi(\Omega_u,t-t',T) \Rightarrow\frac{a_0^2}{2}\sum_{m=1}^{v_{\max}}\sum_{n=0}^{m-1}K_{mn}^2\int_{A_{mn}}^{B_{mn}}d\Omega \times\Phi(\Omega,t-t',T)g_{mn}(\Omega), \tag{28}$$

where $A_{mn}<\omega_{mn}<B_{mn}$. The Bose-Einstein distribution function $\overline{n(}\Omega)$ is approximated in each frequency interval $A_{mn}\leqslant\Omega\leqslant B_{mn}$ by its ''central value'' $\overline{n(}\omega_{mn})$. Assuming also that the reasonable choice of $\gamma_{mn}$ provides small overlap of the neighboring distributions $g_{mn}(\Omega)$, we can set $A_{mn}=-\infty$ and $B_{mn}=\infty$, which yields tabulated integrals [49] in Eq. (28). The final expression for the time correlation function (24) has the form

$$\langle F(t)F(t')\rangle=\frac{a_0^2}{2}\sum_{m=1}^{v_{\max}}\sum_{n=0}^{m-1}K_{mn}^2(\gamma_{mn}/\Omega_0)^p \times\exp(-\gamma_{mn}|t-t'|) \times\{[\overline{n(}\omega_{mn})+1]\exp[-i\omega_{mn}(t-t')] + \overline{n(}\omega_{mn})\exp[i\omega_{mn}(t-t')]\}. \tag{29}$$

Equation (29) will be used for evaluating the time-dependent relaxation matrix (21) in the equation of motion (20) as described below.

In a general case, numerical integration of the integrodifferential equation of motion (20) beyond a Markov-type approximation is an extremely time-consuming task. In the present work, the state-selective preparation of high vibrational bound states as well as dissociation of OH are investigated under the following two assumptions.

(1) The coupling of the dissociation fragments to the environment is not taken into account, which enters the de-

scription by assuming that the respective matrix elements of the molecular coupling operator $Q(r)$ in the basis of molecular eigenstates $|v\rangle$ and $|\varepsilon\rangle$ are zeros:

$$Q_{v\varepsilon}=\langle v|Q|\varepsilon\rangle=0, \quad Q_{\varepsilon' \varepsilon}=\langle \varepsilon'|Q|\varepsilon\rangle=0. \tag{30}$$

This assumption corresponds, for example, to a molecule adsorbed on a surface.

(2) In the second assumption we take into account that the laser-induced continuum-continuum transitions could be safely neglected in a rather wide range of the laser electric-field strength and the carrier frequency [38,39] and set the respective matrix elements of the molecular dipole moment operator $\mu(r)$ to zero:

$$\mu_{\varepsilon' \varepsilon}=\langle \varepsilon'|\mu|\varepsilon\rangle=0. \tag{31}$$

This assumption has been checked in detail for the isolated OH in our recent works [38,39], and in the following we shall use such laser electric-field strengths and the carrier frequencies that the continuum-continuum transitions are indeed of minor importance, at least for the isolated OH.

For numerical integration, the basic equation of motion (20) and the time-dependent relaxation matrix (21) are represented in the basis of molecular eigenstates $|v\rangle$ and $|\varepsilon\rangle$, taking into account Eqs. (30) and (31). Before proceeding, it is suitable to introduce the following notations for the matrix elements:

$$\begin{aligned}
[A,B]^b_{mn}&=\sum_{k=0}^{v_{\max}}(A_{mk}B_{kn}-B_{mk}A_{kn}),\\
(AB)^b_{mn}&=\sum_{k=0}^{v_{\max}}A_{mk}B_{kn},\\
(AB)^b_{m\varepsilon}&=\sum_{k=0}^{v_{\max}}A_{mk}B_{k\varepsilon},\\
[A,B]^b_{\varepsilon' \varepsilon}&=\sum_{k=0}^{v_{\max}}(A_{\varepsilon' k}B_{k\varepsilon}-B_{\varepsilon' k}A_{k\varepsilon}).
\end{aligned} \tag{32}$$

The upper index $b$ in Eq. (32) and in what follows serves to indicate that summation over the bound states only is included, while the lower indexes may include both discrete and continuum states.

The equation of motion for the bound-bound reduced density matrix elements can be written in the form

$$\begin{aligned}
\frac{\partial}{\partial t}\varrho_I(t)_{vv'}=(i/\hbar)\mathcal{E}(t)\Big\{&[\mu_I(t),\varrho_I(t)]^b_{vv'}\\
&+\int_0^{\varepsilon_{\max}}d\varepsilon'[\mu_I(t)_{v\varepsilon'}\varrho_I(t)_{\varepsilon' v'}\\
&-\varrho_I(t)_{v\varepsilon'}\mu_I(t)_{\varepsilon' v'}]\Big\}\\
&-(\Lambda/\hbar)^2[Q_I(t),G_I(t)]^b_{vv'},
\end{aligned} \tag{33}$$

where the upper limit of integration over the continuum energy $\varepsilon$ is set to $\varepsilon_{\max}$ to be detailed below, and the time-dependent relaxation matrix elements $G_I(t)_{kl}$ in the interaction picture have the form

$$\begin{aligned}
G_I(t)_{kl}=\int_0^t dt'\{&\langle F(t)F(t')\rangle[Q_I(t')\varrho_I(t')]^b_{kl}-\langle F(t')F(t)\rangle\\
&\times[\varrho_I(t')Q_I(t')]^b_{kl}\}.
\end{aligned} \tag{34}$$

The initial conditions,

$$\begin{aligned}
&\varrho_I(0)_{v'v}\\
&=\left[\exp(-E_v/k_BT)\Big/\sum_{v''}\exp(-E_{v''}/k_BT)\right]\delta_{v'v},
\end{aligned} \tag{35}$$

correspond to the thermal equilibrium of the molecule and the environment at $T=300$ K.

Equation (33) includes the bound-continuum reduced density matrix elements which are governed by the equation

$$\begin{aligned}
\frac{\partial}{\partial t}\varrho_I(t)_{v\varepsilon}=(i/\hbar)\mathcal{E}(t)\Big\{&[\mu_I(t),\varrho_I(t)]^b_{v\varepsilon}\\
&+\int_0^{\varepsilon_{\max}}d\varepsilon'\mu_I(t)_{v\varepsilon'}\varrho_I(t)_{\varepsilon' \varepsilon}\Big\}\\
&-(\Lambda/\hbar)^2[Q_I(t)G_I(t)]^b_{v\varepsilon},
\end{aligned} \tag{36}$$

where the time-dependent relaxation matrix elements $G_I(t)_{k\varepsilon}$ have the form

$$G_I(t)_{k\varepsilon}=\int_0^t dt'\langle F(t)F(t')\rangle[Q_I(t')\varrho_I(t')]^b_{k\varepsilon}. \tag{37}$$

The initial conditions in Eq. (36) are $\varrho_I(0)_{v\varepsilon}=0$.

Equation (36) includes the continuum-continuum reduced density matrix elements which are governed by the equation

$$\frac{\partial}{\partial t}\varrho_I(t)_{\varepsilon' \varepsilon}=(i/\hbar)\mathcal{E}(t)[\mu_I(t),\varrho_I(t)]^b_{\varepsilon' \varepsilon}, \tag{38}$$

with the initial conditions $\varrho_I(0)_{\varepsilon' \varepsilon}=0$.

The numerical efforts can be reduced drastically by making use of the formal solution of Eq. (38) which has the form

$$\varrho_I(t)_{\varepsilon' \varepsilon}=(i/\hbar)\int_0^t dt'\mathcal{E}(t')[\mu_I(t'),\varrho_I(t')]^b_{\varepsilon' \varepsilon}. \tag{39}$$

Substitution of Eq. (39) into the right-hand side of Eq. (36) yields finally the equation of motion for the bound-continuum reduced density matrix elements

$$\frac{\partial}{\partial t}\varrho_I(t)_{v\varepsilon}=(i/\hbar)\mathcal{E}(t)\Big\{[\mu_I(t),\varrho_I(t)]^b_{v\varepsilon}+(i/\hbar)\int_0^{\varepsilon_{\max}}d\varepsilon'\,\mu_I(t)_{v\varepsilon'}\int_0^t dt'\,\mathcal{E}(t')\times[\mu_I(t'),\varrho_I(t')]^b_{\varepsilon'\varepsilon}\Big\}-(\Lambda/\hbar)^2[Q_I(t)G_I(t)]^b_{v\varepsilon}, \tag{40}$$

where the time-dependent relaxation matrix elements $G_I(t)_{k\varepsilon}$ are defined by Eq. (37).

Equations (33) and (40) are the basic equations of motion in the present work. They constitute the set of coupled integrodifferential equations for the bound-bound and the bound-continuum reduced density matrix elements, including the bound-bound and the bound-continuum matrix elements of operators $\mu_I(r,t)$ and $Q_I(r,t)$ in the interaction picture, which are related to the Schrödinger picture as follows:

$$\langle v|\mu_I(r,t)|v'\rangle=\exp(i\omega_{vv'}t)\mu_{vv'}, \tag{41}$$

$$\langle v|\mu_I(r,t)|\varepsilon\rangle=\exp(i\omega_{v\varepsilon}t)\mu_{v\varepsilon}, \tag{42}$$

$$\langle v|Q_I(r,t)|v'\rangle=\exp(i\omega_{vv'}t)Q_{vv'}. \tag{43}$$

The matrix elements for bound-bound transitions $\mu_{vv'}$ and $Q_{vv'}$ are evaluated, as in our previous work [31], following the methods developed in Refs. [43] and [50], respectively. The matrix elements for bound-continuum transitions $\mu_{v\varepsilon}$ are evaluated as in our recent works [38,39] (details are given in the Appendix of Ref. [39]). Suffice it to note here that for OH under study a strong decrease of the bound-continuum coupling with increasing energy at $\varepsilon>0.05D$, where $D$ is the well depth, allows in our simulations the upper limit of integration over the continuum energy $\varepsilon$ in the basic equations of motion (33) and (40) to be chosen as $\varepsilon_{\max}<0.5D$, with the specific value depending on the laser field strength and the carrier frequency. The integrals over $\varepsilon$ in Eqs. (33) and (40) are approximated with sums, assuming that the $\langle v|\mu|\varepsilon\rangle$ are approximately constant over a series of energy intervals $[\varepsilon_i,\varepsilon_i+\Delta\varepsilon_i]$, where $\Delta\varepsilon_i$ are adjusted to obtain desired accuracy. The size of each energy interval $\Delta\varepsilon_i$ depends on the behavior of the dipole matrix elements $\langle v|\mu|\varepsilon\rangle$ in the vicinity of the discretized continuum energy $\varepsilon_i$. For the evenly discretized continuum energy intervals $\Delta\varepsilon$, for example, convergence of the results is achieved at $\Delta\varepsilon\leqslant 0.00015E_h$.

The time correlation functions in Eqs. (34) and (37) are given by Eq. (29) where, taking into account the spacing between molecular frequencies, we set the parameter $\gamma_{mn}=\Delta^a/2$, which yields the correlation time of the environment $\tau_c\approx 0.7$ ps. Similar to our previous work [31], we set in our computer simulations $p=1$ and choose a scaling parameter $\Omega_0=\omega_{10}$ in Eq. (29). The strength of the molecule-environment coupling is defined in the following by a dimensionless parameter

$$\lambda=(\Lambda a_0^2/\hbar\omega_{10}). \tag{44}$$

The integrodifferential equations (33) and (40) can be solved by using several modifications of standard numerical methods [51]. In the present work we use Adams-Bashforth-Moulton schemes for a predictor-corrector method similar to our previous works [29–31]. The integrals over time $t$ are approximated with sums and calculated on both predictor and corrector steps, with the time step being $\Delta t\leqslant 0.1$ atu. The solution of Eqs. (33) and (40) yields the reduced density matrix elements $\varrho_I(t)_{vv'}$ and $\varrho_I(t)_{v\varepsilon}$. The time-dependent populations of the vibrational bound states are given by

$$P_v(t)=\varrho_I(t)_{vv}, \tag{45}$$

which are of primary importance for investigation of the state-selective phenomena. We shall also use the overall population of all bound states in the well

$$P_{\text{well}}(t)=\sum_{v=0}^{v_{\max}}P_v(t). \tag{46}$$

The populations of the continuum states are represented in this work by integrated quantities

$$P_\varepsilon(t)=\int_{\varepsilon-\Delta\varepsilon/2}^{\varepsilon+\Delta\varepsilon/2}d\varepsilon'\,\varrho_I(t)_{\varepsilon'\varepsilon'}, \tag{47}$$

for the narrow discretized energy interval $\Delta\varepsilon$, and

$$P_{\text{cont}}(t)=\int_0^{\varepsilon_{\max}}d\varepsilon'\,\varrho_I(t)_{\varepsilon'\varepsilon'}, \tag{48}$$

for the overall population of all continuum states, which is equivalent to the dissociation probability $\mathcal{D}(t)=1-P_{\text{well}}(t)$. The explicit form for $\varrho_I(t)_{\varepsilon\varepsilon}$ in Eqs. (47) and (48) is derived from Eq. (39). It is given by the equation

$$\varrho_I(t)_{\varepsilon\varepsilon}=(2/\hbar)\int_0^t dt'\,\mathcal{E}(t')\sum_{k=0}^{v_{\max}}\text{Im}[\varrho_I(t')_{\varepsilon k}\mu_I(t')_{k\varepsilon}], \tag{49}$$

where the reduced density matrix elements $\varrho_I(t)_{\varepsilon k}=\varrho_I(t)^*_{k\varepsilon}$ are obtained from the numerical solution of Eqs. (33) and (40).

To conclude this section, it is worthwhile to note that the basic equations of motion (33) and (40) have been derived within the second-order perturbation theory assuming that the molecule and the environment are uncorrelated [see Eq. (18) and Ref. [48] for details]. In our previous work [31] the applicability of these approximations for the vibrational bound states of OH has been estimated on a picosecond time scale within the fourth-order perturbation theory, where the molecule and the environment have been assumed to be uncorrelated only at the initial time $t$, but not for all times $t>0$. The respective results (see the Appendix in Ref. [31]) are in a good agreement with the non-Markov analysis of the nondissociative state-selective dynamics of OH. A similar non-Markov approach will be used in the next section for

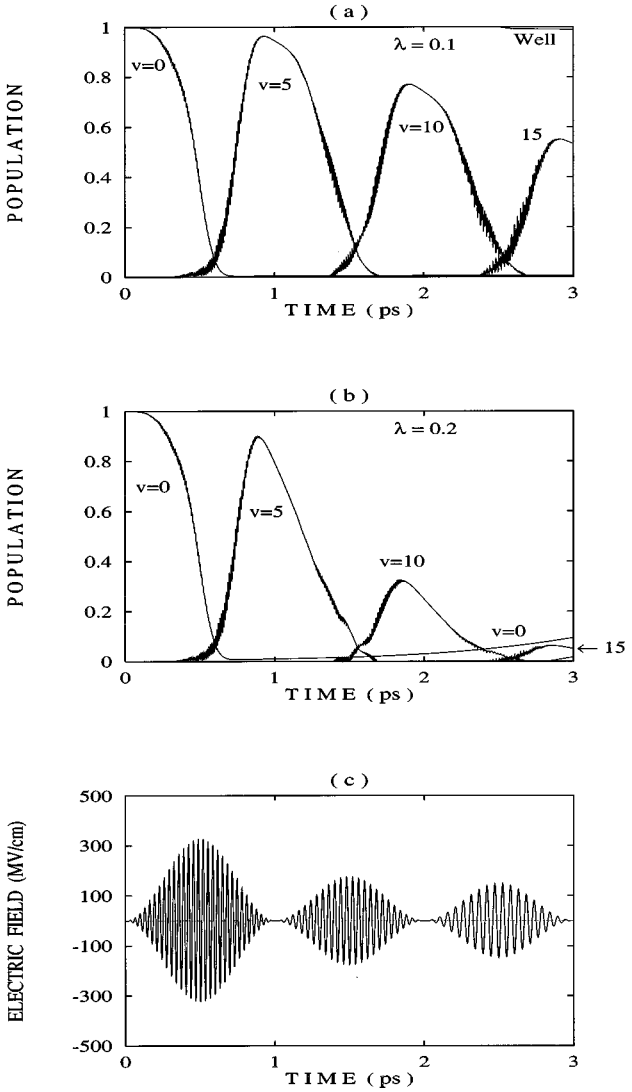


FIG. 1. Selective preparation of vibrational bound state $|v=15\rangle$ of OH by three nonoverlapping 1 ps laser pulses. (a),(b) Population dynamics at different strengths of the molecule-environment coupling λ. Numbers of levels are indicated near the curves, ''Well''—overall population of all bound states. (c) Optimal laser field; the laser pulse parameters: $\mathcal{E}_1^{\rm opt}=328.05$ MV/cm, $\omega_1^{\rm opt}=3424.19$ cm$^{-1}$, $\mathcal{E}_2^{\rm opt}=176.44$ MV/cm, $\omega_2^{\rm opt}=2525.52$ cm$^{-1}$, $\mathcal{E}_3^{\rm opt}=148.07$ MV/cm, $\omega_3^{\rm opt}=1625.67$ cm$^{-1}$.

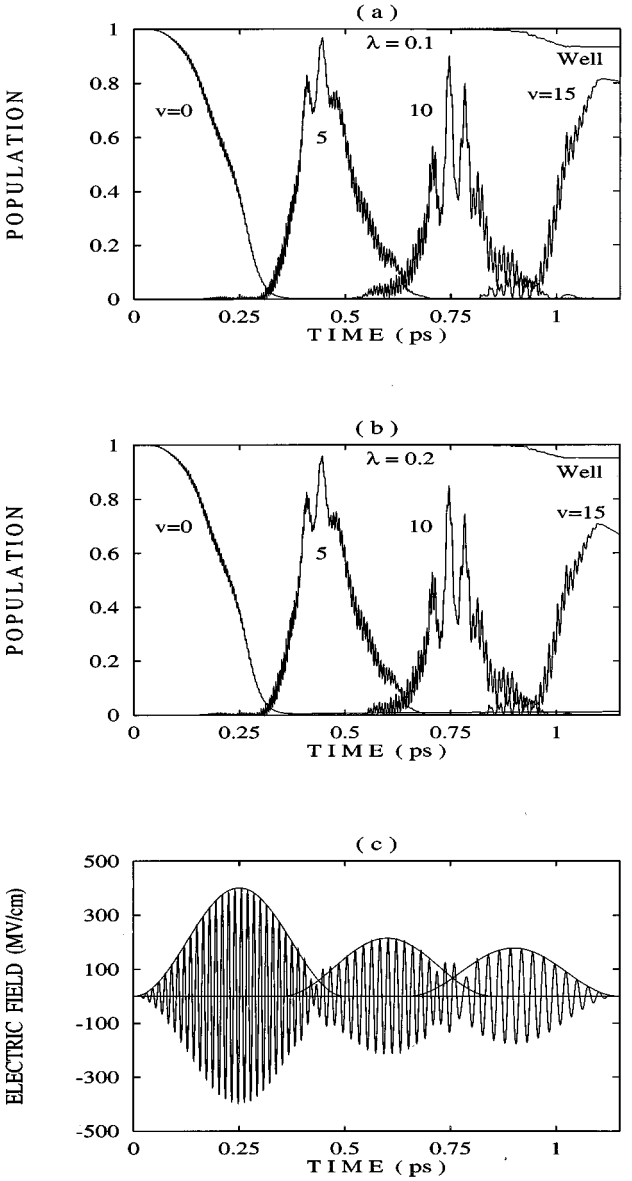


FIG. 2. Selective preparation of vibrational bound state $|v=15\rangle$ of OH by three optimally overlapping 0.5 ps laser pulses. (a),(b) Population dynamics. (c) Optimal laser field; the laser pulse parameters: $\mathcal{E}_1^{\rm opt}=400.75$ MV/cm, $\omega_1^{\rm opt}=3425.79$ cm$^{-1}$, $\mathcal{E}_2^{\rm opt}=214.56$ MV/cm, $\omega_2^{\rm opt}=2524.69$ cm$^{-1}$, $t_{02}^{\rm opt}=0.35$ ps, $\mathcal{E}_3^{\rm opt}=178.21$ MV/cm, $\omega_3^{\rm opt}=1629.83$ cm$^{-1}$, $t_{03}^{\rm opt}=0.65$ ps [$t_{0i}^{\rm opt}$ stands for the optimal time of the beginning of the $i$th laser pulse, see Eq. (50)].

simulations of dissociative dynamics of OH. The applicability of our basic equations of motion (33) and (40) is also restricted to rather small values of the coupling parameter λ defined by Eq. (44), for example, such as used in the next section. Nevertheless, the quasiresonant nature of the environment makes it possible to consider rather fast relaxation rates (see also Refs. [29–31]).

## III. SELECTIVE PREPARATION OF HIGH VIBRATIONAL BOUND STATES AND DISSOCIATION

Excitation of high vibrational bound states by short and strong laser pulses can be accompanied by substantial dissociation unless a special care is taken of optimal design of the laser field to be used for preparing the state selectively. Therefore in the first stage, our aim is to achieve maximal localization of population at a chosen high-lying vibrational bound state $|v\rangle$, along with minimizing the dissociation probability $\mathcal{D}$, while in the second stage, the aim is to achieve maximal dissociation from the selectively prepared high-lying bound state. In both cases the laser-driven molecular dynamics should compete against relaxation.

The laser fields to be used for selective excitation of high vibrational bound states and dissociation of OH may be composed, in general, of several ultrashort pulses with the global electric field strength

$$\mathcal{E}(t)=\sum_i \mathcal{E}_i \sin^2[\pi(t-t_{0i})/t_{pi}]\cos[\omega_i(t-t_{0i})+\varphi_i], \tag{50}$$

where the $i$th laser pulse starts at $t=t_{0i}$, its duration is $t_{pi}$, the electric field amplitude is $\mathcal{E}_i$, and $\omega_i$ is the laser carrier frequency. The phases $\varphi_i$ proved to be of minor importance, and the results below are presented for $\varphi_i=0$. The $\sin^2$ shape of the laser pulses is suitable, but rather arbitrary. Similar results can be obtained by using other ''bell''-type shapes of the pulses, for example, Gaussian [6], or soliton-type, hyperbolic secant shapes [24,52]. With the large vibrational quanta of OH, only the vibrational ground state is substantially populated initially at $T=300$ K, while the population of the first excited state is $P_{v=1}(0)=1.31\times10^{-8}$, for example. Therefore the density matrix elements $\varrho_I(t>0)_{v'v}$ are equal with a very good accuracy to their initial values $\varrho_I(0)_{v'v}\approx\delta_{v'0}\delta_{v0}$ until the laser field is switched on, as has been shown in our previous work [31]. For this reason it is assumed in the following that the laser field is switched on at $t=0$.

The amplitudes $\mathcal{E}_i$, the carrier frequencies $\omega_i$ and the overlaps of individual laser pulses are optimized as described in Refs. [29–31,38,39] in order to achieve a prespecified aim: maximize the population of the target bound state along with minimizing the dissociation probability or, alternatively, maximize the dissociation yield. In order to demonstrate our general approach to the optimal design of the laser field, we choose the bound state $|v=15\rangle$ as a target for state-selective preparation. This state may also serve as a suitable intermediate for selective preparation of the topmost bound states (close to the dissociation threshold) and for efficient dissociation as well. Selective preparation of $|v=15\rangle$ can be achieved, for example, by making use of three laser pulses pumping the sequential five-photon transitions

$$|v=0\rangle\rightarrow(5\ \text{photons})\rightarrow|v=5\rangle\rightarrow(5\ \text{photons})\rightarrow|v=10\rangle\rightarrow(5\ \text{photons})\rightarrow|v=15\rangle. \tag{51}$$

The population dynamics controlled by three nonoverlapping 1 ps laser pulses is shown in Figs. 1(a) and 1(b) for $\lambda=0.1$ and 0.2, respectively. Numbers of bound states are indicated near the curves, curve ''Well'' in Fig. 1(a) gives the overall population of all bound states. The dissociation probability is very small, less than 1% at $\lambda=0.1$, for example. The optimal laser field is shown in the bottom, Fig. 1(c). Note that the three sequential 1 ps laser pulses yield almost complete, more than 95%, population transfer to $|v=15\rangle$ in the absence of relaxation ($\lambda=0$), see Refs. [38,39] for details. At a moderate relaxation, Fig. 1(a), the maximal population of the target bound state is $P_{15}^{\max}=0.55$, while at the strong relaxation, Fig. 1(b), the maximal population $P_{15}^{\max}$ is only 0.06 (even less than population of the initial state $|v=0\rangle$ at the end of the third laser pulse). It is seen from Fig. 1 that while the first (strongest) laser pulse dominates over relaxation, providing rather high population transfer to the intermediate bound state $|v=5\rangle$, weaker laser pulses (the second and the third) cannot efficiently compete against relaxation, especially at the strong molecule-environment coupling ($\lambda=0.2$). Relaxation is also a dominance between the pulses where the laser field is weak.

The laser control over the population dynamics can be much enhanced by making use of shorter and/or overlapping laser pulses. Shorter laser pulses reduce the overall time of the process and require stronger optimal fields, while optimally chosen overlaps increase the electric-field strength between the pulses. All the three factors improve the state-selective laser control of molecular excitation. In Figs. 2(a) and 2(b) the state-selective preparation of $|v=15\rangle$, is demonstrated for the same excitation pathway (51) which is controlled by three overlapping 0.5 ps laser pulses at the same molecule-environment couplings as in Fig. 1 ($\lambda=0.1$ and 0.2). The optimal laser field composed of the three overlapping pulses is shown in Fig. 2(c) together with the $\sin^2$ envelopes of the pulses. It is clearly seen from Fig. 2 that population transfer to the target state $|v=15\rangle$ is remarkably increased, as compared to the case shown in Fig. 1, especially at the strong molecule-environment coupling: the maximal population of the target bound state is $P_{15}^{\max}=0.81$ at $\lambda=0.1$, and $P_{15}^{\max}=0.71$ at $\lambda=0.2$ [more than ten times larger as compared to the respective case of Fig. 1(b)]. The overall populations of the bound states, shown by curves ''Well'' in Figs. 2(a) and 2(b), imply rather small dissociation probabilities: $\mathcal{D}\approx0.07$ and $\mathcal{D}\approx0.05$ at $\lambda=0.1$ and $\lambda=0.2$, correspondingly. Minimization of the dissociation probability is very important for efficient population transfer to high vibrational bound states. Note that the dissociation probability decreases as the coupling of the molecule to the environment increases.

Another possibility of population transfer to the target state $|v=15\rangle$ can be realized (similar to isolated molecules [38,39]) by pumping the overtone transition

$$|v=10\rangle\rightarrow(1\ \text{photon})\rightarrow|v=15\rangle \tag{52}$$

in the third step of the excitation pathway (51). Similar to the previous case, the population transfer is efficient, if short and overlapping laser pulses are used.

On the contrary, the topmost bound states can be prepared selectively only if the overtone transition is pumped in the final step of the overall excitation pathway, while the respective multiphoton pumping can yield efficient dissociation. These issues are demonstrated below for selective preparation of the bound state $|v=20\rangle$ and for multiphoton dissociation of OH via the intermediate bound state $|v=19\rangle$.

Selective preparation of the target bound state $|v=20\rangle$ (i.e., one state before the highest bound state of OH) can be achieved by making use of four laser pulses pumping the sequential resonances according to the following excitation pathway:

$$|v=0\rangle\rightarrow(5\ \text{photons})\rightarrow|v=5\rangle\rightarrow(5\ \text{photons})\rightarrow|v=10\rangle\rightarrow(5\ \text{photons})\rightarrow|v=15\rangle\rightarrow(1\ \text{photon})\rightarrow|v=20\rangle. \tag{53}$$

In our computer simulations we use optimally overlapping 0.5 ps laser pulses. The population dynamics controlled by the four pulses is shown in Figs. 3(a) and 3(b) for $\lambda=0.1$ and 0.2, respectively, where curves ''Well'' give the overall populations of all bound states. The optimal laser field is shown in the bottom, Fig. 3(c), together with the $\sin^2$ envelopes of the four pulses. The maximal population of the target bound state is $P_{20}^{\max}=0.69$ at $\lambda=0.1$ and $P_{20}^{\max}=0.55$ at $\lambda=0.2$. On the contrary, the dissociation probability by the end of the last pulse is fairly small: $\mathcal{D}\approx0.15$ and $\mathcal{D}\approx0.11$ at $\lambda=0.1$, and $\lambda=0.2$, correspondingly. Note that minimization of the dissociation probability is a nontrivial task when preparing the topmost bound states. It is seen from Fig. 3 that

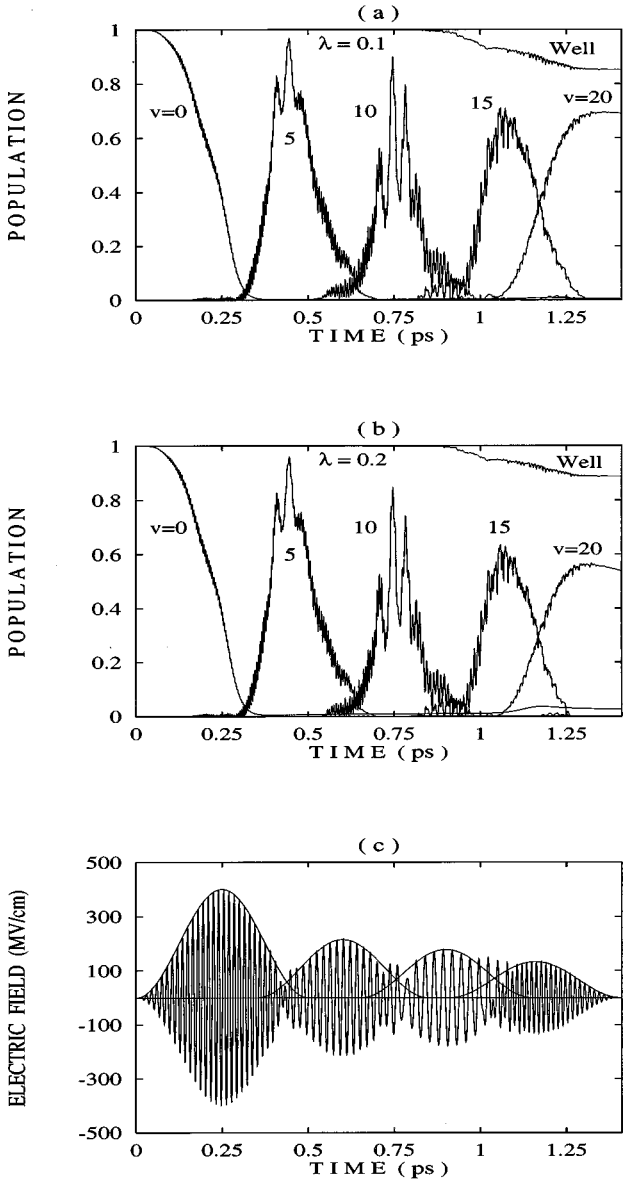


FIG. 3. Selective preparation of vibrational bound state $|v=20\rangle$ of OH by four optimally overlapping 0.5 ps laser pulses. (a),(b) Population dynamics. (c) Optimal laser field; the laser pulse parameters: $\mathcal{E}_1^{\rm opt}=400.75$ MV/cm, $\omega_1^{\rm opt}=3425.79\ cm^{-1}$, $\mathcal{E}_2^{\rm opt}=214.56$ MV/cm, $\omega_2^{\rm opt}=2524.69\ {\rm cm}^{-1}$, $t_{02}^{\rm opt}=0.35$ ps, $\mathcal{E}_3^{\rm opt}=178.21$ MV/cm, $\omega_3^{\rm opt}=1629.83\ {\rm cm}^{-1}$, $t_{03}^{\rm opt}=0.65$ ps, $\mathcal{E}_4^{\rm opt}=132.99$ MV/cm, $\omega_4^{\rm opt}=3663.47\ {\rm cm}^{-1}$, $t_{04}^{\rm opt}=0.91$ ps.

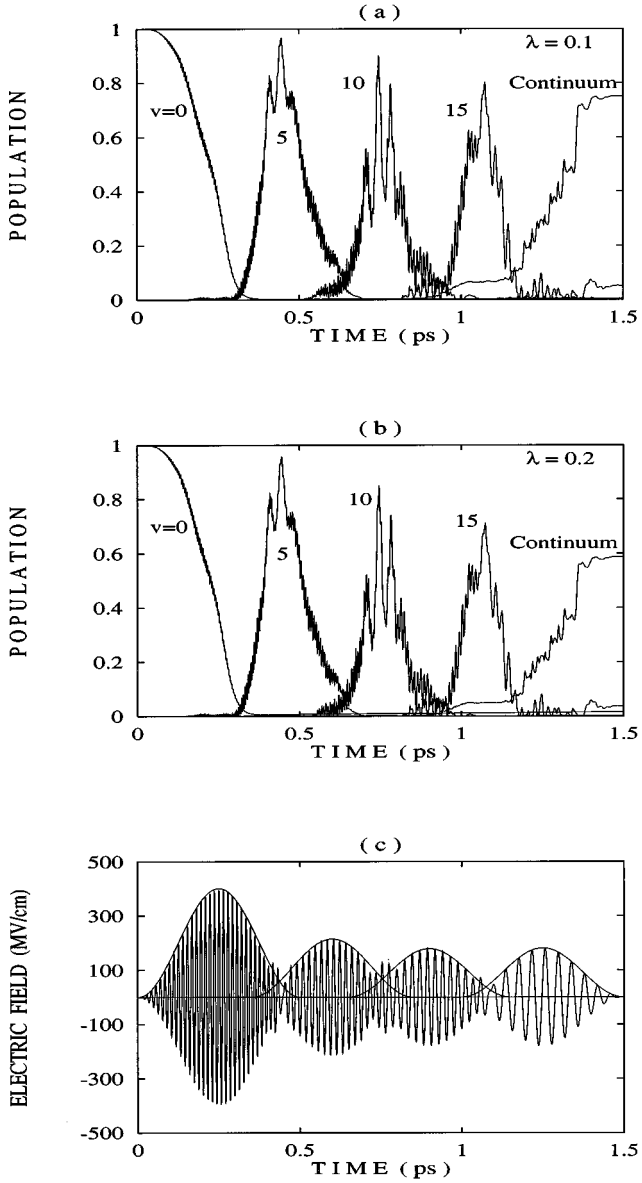


FIG. 4. Multiphoton dissociation of OH by four optimally overlapping 0.5 ps laser pulses. (a),(b) Population dynamics. (c) Optimal laser field; the laser pulse parameters: $\mathcal{E}_1^{\rm opt}=400.75$ MV/cm, $\omega_1^{\rm opt}=3425.79\ {\rm cm}^{-1}$, $\mathcal{E}_2^{\rm opt}=214.56$ MV/cm, $\omega_2^{\rm opt}=2524.69\ {\rm cm}^{-1}$, $t_{02}^{\rm opt}=0.35$ ps, $\mathcal{E}_3^{\rm opt}=178.21$ MV/cm, $\omega_3^{\rm opt}=1629.83\ {\rm cm}^{-1}$, $t_{03}^{\rm opt}=0.65$ ps, $\mathcal{E}_4^{\rm opt}=180.87$ MV/cm, $\omega_4^{\rm opt}=822.464\ {\rm cm}^{-1}$, $t_{04}^{\rm opt}=1$ ps.

even very high vibrational bound states of a molecule coupled to an environment can be prepared selectively, with the probability of about 55–70 %, if the laser field controlling this process is properly shaped and optimized.

For the efficient dissociation of a molecule to be achieved, the overall excitation pathway (53) should be modified in the last step only, for example, as follows. We choose the bound state $|v=19\rangle$ as a higher intermediate state, which being pumped in the vicinity of four-photon resonance from the state $|v=15\rangle$, is spaced by one quantum of photon energy from the continuum states $(\varepsilon-\delta\varepsilon)<\varepsilon<(\varepsilon+\delta\varepsilon)$ which are close to the maximum of the laser-induced bound-continuum coupling represented by the matrix element $\langle v=19|\mu|\varepsilon\rangle$ (see Ref. [39] for details). Therefore the overall dissociation pathway to be controlled by four laser pulses can be schematically presented as

$$\begin{aligned}|v=0\rangle\rightarrow(5\ \ \text{photons})\rightarrow|v=5\rangle\rightarrow(5\ \ \text{photons})\rightarrow|v=10\rangle\\ \rightarrow(5\ \ \text{photons})\rightarrow|v=15\rangle\rightarrow(4\ \ \text{photons})\rightarrow|v=19\rangle\\ \rightarrow(1\ \ \text{photon})\rightarrow\text{``continuum''}.\end{aligned}\tag{54}$$

The population dynamics during the multiphoton dissociation of OH through the pathway (54) controlled by four optimally overlapping 0.5 ps laser pulses is shown in Figs. 4(a) and 4(b) for $\lambda=0.1$ and 0.2, respectively, where curves ''Continuum'' give the overall populations of all continuum states $P_{\rm cont}(t)$ [see Eq. (48)], which is equivalent to the dissociation probability $\mathcal{D}(t)$. The optimal laser field is shown

in the bottom, Fig. 4(c), together with the $\sin^2$ envelopes of the pulses. The overall population of the continuum states at the end of the last laser pulse is $P_{\mathrm{cont}} \approx 0.75$ at $\lambda = 0.1$, and $P_{\mathrm{cont}} \approx 0.59$ at $\lambda = 0.2$, implying an efficient dissociation of a molecule even in the presence of the quasiresonant environment, which reduces the lifetimes of the vibrational bound states into a subpicosecond time domain.

Comparison of the results presented in Figs. 3 and 4 shows that the optimal design of the laser control field can yield either the efficient population transfer to a very high vibrational bound state along with a small dissociation probability (as shown in Fig. 3 for $|v=20\rangle$) or, alternatively, the efficient dissociation of a molecule (as shown in Fig. 4). The overall laser control scheme is basically devided into two stages: in the first stage, a suitable intermediate bound state is prepared selectively (as shown in Fig. 2 for $|v=15\rangle$, for example), while in the second stage, an efficient population transfer to a very high target bound state is achieved by pumping the respective overtone transition, or an efficient dissociation is realized by pumping a suitable multiphoton transition. The series of optimally chosen shaped laser pulses provide a flexible tool for controlling the state-selective molecular dynamics up to the topmost bound states, as well as for efficient dissociation. The overlap of sequential laser pulses is a very important optimization parameter in the overall laser control scheme which, being optimally chosen, significantly increases the population transfer to the target bound state and the dissociation yield.

## IV. CONCLUSION

In the present work the laser-controlled ultrafast state-selective excitation of high vibrational bound states and dissociation of diatomic molecules in an environment has been investigated by means of computer simulation within the reduced density matrix formalism beyond a Markov-type approximation. This work provides the extension of our previous study of the ultrafast population transfer to low and moderately high vibrational bound states where the laser-induced dissociation could be safely neglected [31]. The results of the present work show that very high vibrational bound states of a molecule coupled to an environment, including the bound states close to the dissociation threshold, can be populated selectively on a picosecond time scale with the probability up to 70–80 % or, alternatively, the dissociation yield of about 75% can be achieved, despite the molecule-environment coupling which reduces the lifetimes of the vibrational bound states into a subpicosecond time domain. The optimal laser fields efficiently controlling these processes may include the superposition of up to four subpicosecond shaped laser pulses with properly chosen amplitudes, carrier frequencies and overlaps.

Our computer simulations have been carried out for a one-dimensional dissociative Morse oscillator (a molecule) tailored to the local OH bond in the $H_2O$ and HOD molecules in the ground electronic state. The environment has been represented by an infinite ensemble of harmonic oscillators, with the maximal strength of the molecule-environment coupling corresponding to all molecular frequencies. The quasiresonant molecule-environment coupling assumed in this work, being the most unfavorable condition, has made it possible to study the limits of the ultrafast laser-pulse control of the state-selective dissipative dynamics of diatomic molecules. Therefore, both the 70–80 % population transfer to the topmost bound states and nearly 75% dissociation yield demonstrated in the present work may be substantially higher, if a specific environment is off resonance with the molecular frequencies.

The role of molecular rotation in the presence of an environment requires special investigation. The relevance of one-dimensional to full-dimensional simulations has been discussed recently for the isolated HF in Ref. [40] and specifically for the state-selective population transfer in isolated OH in Ref. [38]. Note also that in the presence of an environment the role of rotation is diminished by the molecule-environment coupling, while the strong linearly polarized laser fields, used in our control schemes for manipulation of the dissipative vibrational dynamics of OH, can induce a substantial degree of molecular alignment [53,54].

The coupling of the dissociation fragments to the environment has not been taken into account in the present study, which corresponds, for example, to a molecule adsorbed on a surface. Note that the aforementioned bound-continuum coupling could rather easily be included in the basic equations of motion (33) and (40) by making use of the respective matrix elements $\langle v|Q|\varepsilon\rangle$, which can be evaluated similar to the bound-continuum matrix elements $\langle v|\mu|\varepsilon\rangle$, as in Ref. [39]. This will make it possible to consider molecular recombination in the gas phase, for example. Our investigations along this line are currently in progress and will be reported in a future work.

The role of the laser-induced continuum-continuum transitions (which have not been taken into account in the present study) has been investigated in detail for the isolated OH previously [38,39], and in the present work we have used such laser electric-field strengths and the carrier frequencies that the continuum-continuum transitions are of minor importance. Suffice it to indicate here that the continuum-continuum transitions can increase the dissociation yield not more than by about 1–2 % in the case of selective preparation of high vibrational bound states [excitation pathway (51) and/or (53)], and therefore they do not practically influence the state-selective population transfer. In the case of multiphoton dissociation [excitation pathway (54)], the continuum-continuum transitions play only a constructive role, because they may increase the dissociation probability by about 10%, at least for the isolated OH. Note also, that taking account of the laser-induced continuum-continuum transitions seems not to be practicable in the energy representation used in this work. The coordinate space representation may prove to be more suitable, but it requires the development of the respective efficient numerical methods beyond a Markov-type approximation.

## ACKNOWLEDGMENTS

We would like to thank Professor J. Manz for helpful discussions. The present research was supported by the Volkswagen-Stiftung, Project No. I/69 348, which is gratefully acknowledged. The computer simulations were carried out on HP 9000/S 750 workstations at the Freie Universität Berlin.

[1] D. M. Larsen and N. Bloembergen, Opt. Commun. **17**, 254 (1976).
[2] G. K. Paramonov and V. A. Savva, Phys. Lett. **97A**, 340 (1983).
[3] G. K. Paramonov, V. A. Savva, and A. M. Samson, Infrared Phys. **25**, 201 (1985).
[4] U. Gaubatz, P. Rudecki, M. Becker, S. Schiemann, M. Kulz, and K. Bergmann, Chem. Phys. Lett. **149**, 463 (1988).
[5] U. Gaubatz, P. Rudecki, S. Schiemann, and K. Bergmann, J. Chem. Phys. **92**, 5363 (1990).
[6] W. Jakubetz, B. Just, J. Manz, and H.-J. Schreier, J. Phys. Chem. **94**, 2294 (1990).
[7] R. Judson, K. Lehmann, W. S. Warren, and H. Rabitz, J. Mol. Struct. **223**, 425 (1990).
[8] G. K. Paramonov, Phys. Lett. A **152**, 191 (1991).
[9] J. S. Melinger, A. Hariharan, S. R. Gandhi, and W. S. Warren, J. Chem. Phys. **95**, 2210 (1991).
[10] B. W. Shore, K. Bergmann, J. Oreg, and S. Rosenwaks, Phys. Rev. A **44**, 7442 (1991).
[11] B. Just, J. Manz, and G. K. Paramonov, Chem. Phys. Lett. **193**, 429 (1992).
[12] J. S. Melinger, S. R. Gandhi, A. Hariharan, J. X. Tull, and W. S. Warren, Phys. Rev. Lett. **68**, 2000 (1992).
[13] J. Oreg, K. Bergmann, B. W. Shore, and S. Rosenwaks, Phys. Rev. A **45**, 4888 (1992).
[14] B. W. Shore, K. Bergmann, A. Kuhn, S. Schiemann, J. Oreg, and J. H. Eberly, Phys. Rev. A **45**, 5297 (1992).
[15] A. Kuhn, G. W. Coulston, G. Z. He, S. Schiemann, K. Bergmann, and W. S. Warren, J. Chem. Phys. **96**, 4215 (1992).
[16] G. K. Paramonov, Chem. Phys. **177**, 169 (1993).
[17] W. Jakubetz, E. Kades, and J. Manz, J. Phys. Chem. **97**, 12 609 (1993).
[18] J. Manz and G. K. Paramonov, J. Phys. Chem. **97**, 12 625 (1993).
[19] H.-P. Breuer and M. Holthaus, J. Phys. Chem. **97**, 12 634 (1993).
[20] W. Gabriel and P. Rosmus, J. Phys. Chem. **97**, 12 644 (1993).
[21] S. Schiemann, A. Kuhn, S. Stuerwald, and K. Bergmann, Phys. Rev. Lett. **71**, 3637 (1993).
[22] M. Holthaus and B. Just, Phys. Rev. A **49**, 1950 (1994).
[23] G. K. Paramonov, in *Femtosecond Chemistry*, edited by J. Manz and L. Wöste (Verlag Chemie, Weinheim, 1995), Vol. 2, pp. 671–712.
[24] J. S. Melinger, D. McMorrow, C. Hillegas, and W. S. Warren, Phys. Rev. A **51**, 3366 (1995).
[25] D. Malzahn and V. May, Chem. Phys. **197**, 205 (1995).
[26] O. Kühn, D. Malzahn, and V. May, Int. J. Quantum Chem. **57**, 343 (1996).
[27] M. Shapiro, Phys. Rev. A **54**, 1504 (1996).
[28] J. Martin, B. W. Shore, and K. Bergmann, Phys. Rev. A **54**, 1556 (1996).
[29] M. V. Korolkov, J. Manz, and G. K. Paramonov, J. Phys. Chem. **101**, 13 927 (1996).
[30] M. V. Korolkov, J. Manz, and G. K. Paramonov, J. Chem. Phys. **105**, 10 874 (1996).
[31] M. V. Korolkov and G. K. Paramonov, Phys. Rev. A **55**, 589 (1997).
[32] N. Bloembergen and A. H. Zewail, J. Phys. Chem. **88**, 5459 (1984).
[33] J. Manz and C. S. Parmenter, Chem. Phys. **139**, 1 (1989).
[34] J. E. Combariza, B. Just, J. Manz, and G. K. Paramonov, J. Phys. Chem. **95**, 10 351 (1991).
[35] J. E. Combariza, J. Manz, and G. K. Paramonov, Faraday Discuss. Chem. Soc. **91**, 358 (1991).
[36] *Femtosecond Chemistry*, edited by J. Manz and L. Wöste (Verlag Chemie, Weinheim, 1995), Vols. 1,2.
[37] G. K. Paramonov, Chem. Phys. Lett. **250**, 505 (1996).
[38] M. V. Korolkov, Yu. A. Logvin, and G. K. Paramonov, J. Phys. Chem. **100**, 8070 (1996).
[39] M. V. Korolkov, G. K. Paramonov, and B. Schmidt, J. Chem. Phys. **105**, 1862 (1996).
[40] M. Kaluža, J. T. Muckerman, P. Gross, and H. Rabitz, J. Chem. Phys. **100**, 4211 (1994).
[41] M. Kaluža and J. T. Muckerman, J. Chem. Phys. **105**, 535 (1996).
[42] S. Flügge, *Practical Quantum Mechanics* (Springer-Verlag, New York, 1974).
[43] M. L. Sage, Chem. Phys. **35**, 375 (1978).
[44] J. T. Broad, Phys. Rev. A **26**, 3078 (1982).
[45] R. Mecke, Z. Elektrochem. **54**, 38 (1950).
[46] R. T. Lawton and A. S. Child, Mol. Phys. **40**, 773 (1980).
[47] J. A. White and S. Velasco, Chem. Phys. Lett. **164**, 77 (1989).
[48] K. Blum, *Density Matrix Theory and Applications* (Plenum, New York, 1989).
[49] I. S. Gradshteyn and I. M. Ryzhik, *Table of Integrals, Series, and Products* (Academic, New York, 1980).
[50] J. N. Huffaker and L. B. Tran, J. Chem. Phys. **76**, 3838 (1982).
[51] W. H. Press, B. P. Flannery, S. A. Teukolsky, and W. T. Vetterling, *Numerical Recipes* (Cambridge University Press, Cambridge, 1986).
[52] Z. E. Dolya, N. B. Nazarova, G. K. Paramonov, and V. A. Savva, Chem. Phys. Lett. **145**, 499 (1988).
[53] B. Friedrich and D. Herschbach, Phys. Rev. Lett. **74**, 4623 (1995).
[54] T. Seideman, J. Chem. Phys. **103**, 7887 (1995).